WT-1116 (EX)
EXTRACTED VERSION

OPERATION TEAPOT

Project 2.2
Neutron Flux Measurements

February-May 1955

Nevada Test Site

NOTICE

This is an extract of Operation TEAPOT, which remains classified SECRET/RESTRICTED DATA as of this date.

Extract version prepared for:

Director
DEFENSE NUCLEAR AGENCY
Washington, D.C. 20305

1 January 1981

Approved for public release; distribution unlimited.

UNCLASSIFIED

SECURITY CLASSIFICATION OF THIS PAGE (When Data Entered)

REPORT DOCUMENTATION PAGE

READ INSTRUCTIONS BEFORE COMPLETING FORM

1. REPORT NUMBER: WT-1116 (EX) (18) DOE	2. GOVT ACCESSION NO.: AD-A995 088
3. RECIPIENT'S CATALOG NUMBER:	
4. TITLE (and Subtitle): Operation TEAPOT - Project 2.2, Neutron Flux Measurements. (6)	5. TYPE OF REPORT & PERIOD COVERED:
	6. PERFORMING ORG. REPORT NUMBER: WT-1116 (EX)
7. AUTHOR(s): (10) T. D. Hanscome, D. K. Willet	8. CONTRACT OR GRANT NUMBER(s): (11) 1 Jan 61
9. PERFORMING ORGANIZATION NAME AND ADDRESS: Headquarters Field Command, Armed Forces Special Weapons Project, Sandia Base, Albuquerque, New Mexico (9)	10. PROGRAM ELEMENT, PROJECT, TASK AREA & WORK UNIT NUMBERS: Rept. - Feb-May 55
11. CONTROLLING OFFICE NAME AND ADDRESS: (12) 42	12. REPORT DATE: July 28, 1958
	13. NUMBER OF PAGES: 44
14. MONITORING AGENCY NAME & ADDRESS (if different from Controlling Office):	15. SECURITY CLASS. (of this report): Unclassified
	15a. DECLASSIFICATION/DOWNGRADING SCHEDULE:

16. DISTRIBUTION STATEMENT (of this Report)

Approved for public release; unlimited distribution.

17. DISTRIBUTION STATEMENT (of the abstract entered in Block 20, if different from Report)

(15)

18. SUPPLEMENTARY NOTES

This report has had the classified information removed and has been republished in unclassified form for public release. This work was performed by the General Electric Company-TEMPO under contract DNA001-79-C-0455 with the close cooperation of the Classification Management Division of the Defense Nuclear Agency.

19. KEY WORDS (Continue on reverse side if necessary and identify by block number)

Operation TEAPOT
Neutron Flux Measurements

20. ABSTRACT (Continue on reverse side if necessary and identify by block number)

DD FORM 1 JAN 73 1473 EDITION OF 1 NOV 65 IS OBSOLETE

UNCLASSIFIED

FOREWORD

This report has had classified material removed in order to make the information available on an unclassified, open publication basis, to any interested parties. This effort to declassify this report has been accomplished specifically to support the Department of Defense Nuclear Test Personnel Review (NTPR) Program. The objective is to facilitate studies of the low levels of radiation received by some individuals during the atmospheric nuclear test program by making as much information as possible available to all interested parties.

The material which has been deleted is all currently classified as Restricted Data or Formerly Restricted Data under the provision of the Atomic Energy Act of 1954, (as amended) or is National Security Information.

This report has been reproduced directly from available copies of the original material. The locations from which material has been deleted is generally obvious by the spacings and "holes" in the text. Thus the context of the material deleted is identified to assist the reader in the determination of whether the deleted information is germane to his study.

It is the belief of the individuals who have participated in preparing this report by deleting the classified material and of the Defense Nuclear Agency that the report accurately portrays the contents of the original and that the deleted material is of little or no significance to studies into the amounts or types of radiation received by any individuals during the atmospheric nuclear test program.

SUMMARY OF SHOT DATA, OPERATION TEAPOT

Shot	Code Name	Date	Time*	Area	Type	Latitude and Longitude of Zero Point
1	Wasp	18 February	1200	T-7-4†	762-ft Air	37° 05' 11.6856" 116° 01' 18.7366"
2	Moth	22 February	0545	T-3	300-ft Tower	37° 02' 52.2854" 116° 01' 15.6967"
3	Tesla	1 March	0530	T-9b	300-ft Tower	37° 07' 31.5731" 116° 02' 51.0077"
4	Turk	7 March	0520	T-2	500-ft Tower	37° 06' 18.4044" 116° 07' 03.1679"
5	Hornet	12 March	0520	T-3a	300-ft Tower	37° 02' 25.4043" 116° 01' 31.3674"
6	Bee	22 March	0505	T-7-1a	500-ft Tower	37° 05' 41.3880" 116° 01' 25.5474"
7	ESS	23 March	1230	T-10a	67-ft Underground	37° 10' 06.1203" 116° 02' 37.7010"
8	Apple	29 March	0455	T-4	500-ft Tower	37° 05' 43.9200" 116° 06' 09.9040"
9	Wasp'	29 March	1000	T-7-4‡	740-ft Air	37° 05' 11.6856" 116° 01' 18.7366"
10	HA	6 April	1000	T-5§	36,620-ft MSL Air	37° 01' 43.3642" 116° 03' 28.3624"
11	Post	9 April	0430	T-9c	300-ft Tower	37° 01' 19.6965" 116° 02' 03.8869"
12	MET	15 April	1115	FF	400-ft Tower	36° 47' 52.6887" 115° 55' 44.1086"
13	Apple 2	5 May	0510	T-1	500-ft Tower	36° 03' 11.1095" 116° 06' 09.4837"
14	Zucchini	15 May	0500	T-7-1a	500-ft Tower	37° 05' 41.3880" 116° 01' 25.5474"

* Approximate local time, PST prior to 24 April, PDT after 24 April.
† Actual zero point 36 feet north, 426 feet west of T-7-4.
‡ Actual zero point 94 feet north, 62 feet west of T-7-4.
§ Actual zero point 36 feet south, 397 feet west of T-5.

ABSTRACT

The purpose of this project was to measure the neutron energy spectrum as a function of distance and to compare the data obtained with the predictions of neutron flux based upon similar devices detonated under similar conditions. Primary emphasis was placed on measurements on Shots 9 and 10 and on weapons of essentially new design.

Detectors employing gold, sulfur, plutonium, neptunium, and uranium-238 were employed. These detectors were exposed to the neutron fluxes from selected shots and were recovered by removing the cable to which they were attached or by removing them from the canisters as was the case of the Shot 10 detonation.

The gold and sulfur data for Shots 1, 9, and 10 show irregular points. Shots 9 and 10 appear to be nearly alike as neutron sources, but the data for Shot 10 show wide fluctuations for all detectors at close range. This inconsistency is inexplicable.

The results from Shots 3 and 11 show [redacted] asymmetry. Both devices gave higher fluxes than expected.

Shot 12 gave results approximately as expected. It is important to observe the much-higher neutron flux in the energy range between 200 ev and 3 mev, as compared with the gold and sulfur fluxes.

FOREWORD

This report presents the final results of one of the 56 projects comprising the Military Effects Program of Operation Teapot, which included 14 test detonations at the Nevada Test Site in 1955.

For overall Teapot military-effects information, the reader is referred to the "Summary Report of the Technical Director, Military Effects Program," WT-1153, which includes the following: (1) a description of each detonation including yield, zero-point location and environment, type of device, ambient atmospheric conditions, etc.; (2) a discussion of project results; (3) a summary of the objectives and results of each project; (4) a listing of project reports for the Military Effects Program.

CONTENTS

Chapter 1
INTRODUCTION

1.1 OBJECTIVE

The general purpose of Project 2.2 was to measure the neutron energy spectrum as a function of distance from the atomic detonations at Operation TEAPOT and to compare the data obtained with the predictions of neutron flux based on similar devices detonated under similar conditions. Primary emphasis was placed on measurements of identical devices detonated at 800 ft and 40,000 ft heights and on devices of essentially new design. Because biological studies have shown that supra-lethal radiation doses can have immediate effect on co-ordination to a disabling extent, measurements are desired in the region where such doses are predicted. An estimate of the "kill" volume can be made in terms of the biological kill criterion and the flux versus range data.

Specifically (in estimated order of importance) the measurements required were as follows:

1. Neutron flux as a function of distance (at the altitude of the burst) for a nuclear device of several KT yield detonated at 40,000 ft altitude (MSL). The measurements were to be made at slant ranges covering a dose range from 25,000 rem to 25 rem. Figure 1.1 gives the dose predictions in the range of interest.

2. Neutron flux as a function of distance from a device identical to that used for the high-altitude Shot 10, but detonated at 800 ft above the surface. This measurement was to provide data to correlate with Shot 10 to provide a field calibration of the instrumentation used. Shot 10 and the correlation shot (Shot 9) were to provide experimental data on the variation in neutron flux with altitude of the detonation.

3. Neutron flux as a function of distance on developmental devices, [redacted] types.

4. Neutron flux inside and outside selected structures and field fortifications in support of radiation-shielding studies conducted by Project 2.7.

1.2 BACKGROUND AND THEORY

It has been shown empirically that the neutrons from thermal fission have an energy distribution that can be fitted by the function

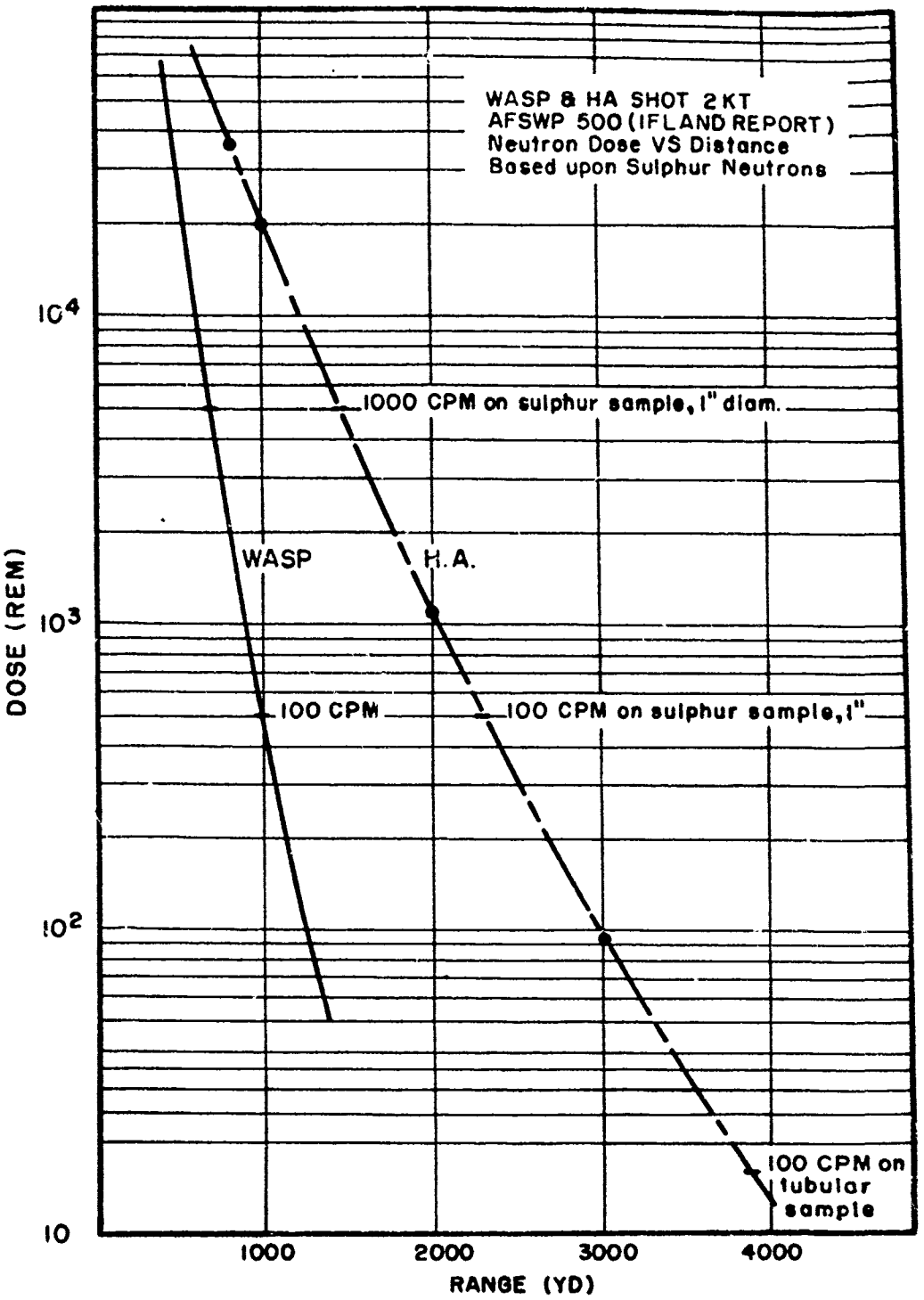

Figure 1.1 Predicted dose versus range for WASP and HA showing sulfur counting rates

$$e^{-x} \sinh \sqrt{2x},$$

where x is proportional to the neutron energy (B. E. Watt, P. R., 87, 1037 (1952)).

Measurements of neutron flux have been made at nearly all previous weapons tests. The completeness of coverage has varied a great deal. Many of the measurements at previous shots have been made for diagnostic purposes. Thus, the spectrum coverage varies widely from shot to shot. The measurements have been made by several laboratories using essentially similar techniques. For a more comprehensive discussion of past measurements the reader is referred to: LAMS-218, LA-361, LA-362, LA-367, LA-1012, LA-1013, (Trinity); XRD-209 (Crossroads); SS-18, SS-18 Add (Sandstone); WT-37, WT-68, WT-96, WT-97, (Greenhouse); WT-202, WT-203, (Ranger); WT-416, WT-424, (Buster/Jangle); WT-524, WT-528, WT-550, WT-555, WT-564, (Tumbler/Snapper); WT-620, WT-621, WT-625, (Ivy); WT-707, WT-720, WT-803, WT-804, (Upshot/Knothole); WT-914, (Castle). These reports give a comprehensive coverage of neutron measurements for both effects and diagnostic purposes. They give the wide range of variation in techniques required for neutron measurements to cover ranges of yield, spectrum and ambient conditions.

Chapter 2
PROCEDURE

Since the neutron radiation from a nuclear weapon is prompt, electronic methods of spectrum analysis are complex and indirect. In principle, threshold detectors provide an ideal method for flux and spectrum measurements. However, the requirements at field tests limit the variety of detectors useful for field work.

2.1 CHOICE AND PREPARATION OF SAMPLES

The choice of materials is limited to those having thresholds in a region of interest. The resulting radioactivity must have a half life long enough to permit reasonable delay in recovery, yet short enough to permit positive identification of the activity in a reasonably short time. In general, half lives greater than 50 hours and shorter than 500 hours are suitable.

Gold was chosen as a slow-neutron detector. By exposing duplicate pieces, one shielded with a 0.045-in. thickness of cadmium, the integrated neutron flux below the cadmium "cutoff" at about 0.3 ev can be measured. The gold samples are 1/2-in.-diameter discs 0.010 in. thick. The gold used was mint gold, 99.99 percent fine. There are no observable interfering activities in gold.

Sulfur has an effective threshold for the $S^{32}(n,p)P^{32}$ reaction at about 3 Mev. Flowers of sulfur (USP resublimed) was used. Three-gram pellets 1-in.-diameter and approximately 1/8 in. thick were prepared in a die at a pressure of 10,000 psi. Each field sample consisted of a polythene bag containing a pellet and about 60 grams of USP flowers of sulfur. In the event that the pellet activity was too low to count, a cylinder was cast using 40 grams of the irradiated sulfur to give almost a 2π solid angle, thereby increasing the counting rates.

Fission threshold detectors were prepared by the Oak Ridge National Laboratory (ORNL) for use by Project 2.2 and others at TEAPOT.

Plutonium can be used as a fission threshold detector, if thermal neutrons causing fission are shielded out with B^{10}. Its effective threshold depends on the thickness of B^{10} used and can be varied from about 200 ev to 4 kev. The samples consist of approximately 1 gram of plutonium foil enclosed in copper foil. The fission-fragment activity can be calibrated in terms of the integrated flux interacting with the sample.

Neptunium has a neutron fission threshold in the region of 700 kev. Samples are prepared by electrodeposition of milligram quantities. More extensive shielding with cadmium is required to prevent interference by the (n,γ) thermal activation cross section, $Np^{237}(n,\gamma)Np^{238}$. The extra shielding against thermal neutrons does not affect the calibration of the plutonium except for the small absorption of epi-

thermal neutrons by the cadmium. The cadmium thickness was chosen to reduce the Np^{238} activity to a tolerable level. Neptunium-238 has a 2.1 day half life, which interferes with the measurement of the activity of the fission fragments.

Uranium-238 has a threshold for neutron fission at 1.4 Mev. The short life of the activation product, U^{239}, makes shielding easy for this material. The U^{239} activity does not interfere because it will have decayed to very low levels by the time the fission fragments activity can be counted.

2.2 EXPERIMENTAL PLANS

The scope of participation (see Table 2.1) was based on the military requirements for comparison of devices in the light of Shot 10. Although few of the devices to be tested were related to Shot 10, it was considered desirable to plan for most of them. Table 2.2 gives some information on the physical features of the devices that affect the neutron flux.

In preparation for Shot 10, a dry run was planned to test dropping and recovery plans. For Shot 10, fifteen canisters provided by Bendix under contract to the Air Force Cambridge Research Center (AFCRC) were instrumented with sulfur, gold, and fission detectors. Initial plans called for dropping intervals of 500 ft close to the bomb and 1,000 ft farther out. Other considerations changed these intervals considerably. The device selected for Shot 10 was to be tested at Shot 1. A detector line and several canisters supported on poles were used at this shot. The second choice for Shot 10 was the Shot 9 device, for which the same instrumentation was used.

Sulfur and gold detectors were used during Shot 6. Fission detectors were used by ORNL in support of other projects.

Gold, [illegible] fission detectors were used. Samples were supplied to Project 2.7 for the instrumentation of foxholes.

Sulfur and gold were exposed on single lines by Project 2.2 during Shots 2 and 5. Fission detectors were exposed by ORNL for other projects.

A detector line was used during Shot 12. Gold and sulfur samples were supplied to Project 2.7 for field-fortification studies. Fission detectors were included in the Shot 12 line and at several fortifications.

A gold and sulfur detector line was used during Shot 8 but not during Shot 13. Gold and sulfur samples were supplied to Project 39.1 for Shots 8 and 13. Fission detectors were desired, but not available for these shots.

2.3 OPERATIONAL PLAN

Early recovery is a prime necessity for the fission-threshold detectors. For this reason, field installations were designed for fast

TABLE 2.1 - PARTICIPATION

Shot	Gold		Fission	Type of Line	Range (yd)	Remarks
1	40		10	Stake	100-1,100	5 canisters
2	11		10	Stake	100-1,200	
3	5		3	Stake	300-1,000	0° to axis
	5		3	Stake	300-1,000	45° to axis
	9		4	Stake	300-1,600	90° to axis
5	10		10	Cable and Stake	100-800	12 sets to 39.1
6	9		10	Cable	200-1,000	12 sets to 39.1
8	10			Cable and Stake	400-2,200	25 sets to 39.6
9	12		12	Cable and Stake	100-1,400	5 canisters
10	90		15	Canisters	250-4,200	
11	5		3	Stake	400-1,200	90° to axis
	5		3	Stake	400-1,200	45° to axis
	10		4	Cable and Stake	300-1,200	0° to axis
12	10		13	Cable	200-1,200	100 sets 2.7.1

TABLE 2.2 - CONFIGURATION OF TEST DEVICES

Shot	Code Name		Yield (KT)
1	WASP		1.2
2	MOTH		2.5
3	TESLA		70
5	HORNET		3.6
6	BEE		8.1
9	WASP'		3.2
10	HA		3.0
11	POST		11.0
12	MET.		24

recovery in order that recoveries could be made in high residual radiation fields. For the shots at which prohibitively high residual radiation was expected, the detectors were fastened to a 3/4-in. cable running from 100 yd from ground zero out to approximately 1,000 vd. The cable was pulled out of the "hot" region and samples removed when it reached a "cool" area.

When low residual radiation was predicted, and relatively low overpressures anticipated, the samples were mounted on a simple stake arrangement. The close-in stations consisted of a 2-in. steel stake with a quick-disconnect crossbar to which the samples were attached. At ranges greater than 600 yd, a 3/4-in. steel stake was used, and the samples were recovered by pulling the stake from the ground.

The sulfur and gold detectors were contained in steel holders provided with a mounting web. The holders were secured to either the 3/4-in. cable or steel stake by means of a cable clamp through the mounting web. The gold holders were 1/4-in. steel plates with cavities milled in one plate to hold the gold discs and cadmium shields. The sulfur holders were 1 1/2-in. pipe nipples 6 in. long, enclosed on both ends with pipe caps. The sulfur was contained in polythene bags which were slipped into the holders.

The fission detectors were encased in spherical steel holders containing the boron shielding with the detectors mounted in a central cavity. These holders were provided with a mounting web and U-bolt for installation.

The samples used in Shot 10 were mounted at two levels in the canisters. The first level held a ring of six gold samples and three sulfur samples. This multiple installation was used to show canister orientation at the time of burst. The self shielding effect in the gold detectors (i.e., higher activity on the side of the gold foil facing the neutron source) resulted in a variation in activity between the top and bottom of a sample and from sample to sample. By observing the top-to-bottom counting ratio and plotting this ratio as a function of sample position in the canister, the direction to the burst appears as a maximum in the polar plot of this ratio. The fission-detector sphere was mounted on a plate several inches below the sulfur and gold. Both installations were secured to common brackets in the canisters for ease of removal.

Canisters were installed on posts for Shots 1 and 9 in an effort to find the effect of the canister construction on the flux recorded by the detectors. These calibration trials showed that the effect of the 3/8-in. steel canister walls was a lowering of the measured flux by about 10 percent.

As a further check on this effect, a calibration run was planned using the Tower Shielding Facility reactor at Oak Ridge. Scheduling difficulties prevented accomplishing this calibration.

The field installations were of two general types, cable and stake lines. The 3/4-in. steel cables were run from 100 yd to 1,000 yd, with stations every hundred yards. The samples were mounted directly on the cable with cable clamps. The samples were kept off the ground to minimize ground scattering by draping the cable across wooden tripods about 4 ft high, care being taken to orient the samples toward the point of burst.

Each stake station consisted of a single 2-in. steel stake to

which an 18-in. crossbar was clamped. Recovery was effected by removing the crossbar to which the samples were fastened.

At Shot 1 Project 2.2 shared stations with the LASL Biomedical group. These stations were placed along a curve so that the heavy biomedical shields could be used at other shots.

Table 2.1 lists the types and numbers of samples exposed for each shot and the ranges over which these samples were spread. Ranges to intended GZ were measured, but angles to GZ were not measured. This was not discovered until after the test when data was sought from the contractor and from LASL.

2.4 COUNTING AND ANALYSIS

Following exposure, the active samples (except for the fission detectors) were flown back to the U. S. Naval Research Laboratory (NRL) for counting and analysis. The calibration of the fission detectors requires counting at a particular time after exposure in order to compare counting rates at the calibrated time. Since good sensitivity requires early counting, the fission detectors were counted by ORNL personnel in a mobile counting laboratory stationed at the control point. For detectors other than the fission samples, the procedure followed is one of establishing the counting rate immediately following exposure and, by means of a suitable calibration number, converting this counting rate data to integrated neutron flux. Much of the counting technique and equipment used is described in earlier test reports (WT-524, WT-720, and WT-914).

2.4.1 Activation Detector, Gold. The reaction of interest is $Au^{197}(n,\gamma)Au^{198}$, characterized by a 64.6-hour beta activity. This detector has been calibrated in a "Sigma" pile at Los Alamos, by exposing the gold samples (bare and cadmium shielded) in their field holder geometry to the accurately known flux of the pile. The calibration samples were then counted in the NRL counter geometry and a calibration number determined. This calibration number is 8.13×10^5 neutrons per count per minute ± 6 percent.

In calculating the integrated neutron flux, the counting rate at any time, t, following exposure, is extrapolated back to the counting rate at the time of exposure, t_o, by the following equation.

$$CR_{t_o} = CR_t \, e^{\lambda (t-t_o)}$$

where CR_{t_o} and CR_t are the counting rates at the respective times and λ is the disintegration constant for the activity in question.

$$\lambda = \frac{0.693}{T_{\frac{1}{2}}} = 1.788 \times 10^{-4} \text{ per minute}$$

The initial counting rates (CR_{t_o}) for both shielded and bare samples are calculated and the neutron flux is calculated as follows:

$$nvt = (CR_{t_o\,bare} - 1.025\ CR_{t_o\,shielded}) \times 8.13 \times 10^5 \text{ neutrons/cm}^2.$$

The factor 1.025 is a correction for epithermal neutrons absorbed by the cadmium.

The activity in the gold foils was counted in continuous-gas-flow proportional counters, using pure methane as the counter gas. These counters have an operating voltage of 4,200 volts with a 500-volt plateau. The counters are of the windowless type and have very nearly 2π geometry. In conjunction with these counters, a decade scaler with a self contained linear amplifier and 1 μsec input circuit is used. In order to eliminate the mechanical registers of these scalers, and thereby increase the maximum counting rate of the unit, "glow tube" registers were substituted in two of the four counting systems. The resolving time is 6 μsec.

Because many of the activated samples were quite "hot" and yielded high counting rates, it was necessary to make count loss corrections. In some cases it was necessary to wait several half lives to get even a correctable count. With the correction curves derived, it was possible to make corrections of 50 percent or more with reasonable accuracy. In general, samples were permitted to cool until the rates were less than 50,000 counts per second.

2.4.2 $S^{32}(n,p)P^{32}$ Threshold Detector. The reaction $S^{32}(n,p)P^{32}$ has a threshold at 1.1 Mev. Because of a resonance just above this threshold, the cross section rises more rapidly than predicted from the penetrability of the emitted proton. It is this feature that makes sulfur a good threshold detector. The cross section rises to 50 millibarns at 2.5 Mev and reaches 100 millibarns at about 3.0 Mev. The "effective" threshold for this reaction will depend on the spectrum. For a fission spectrum the effective threshold is about 3 Mev. Neutrons from the $D(t,n)He^4$ reaction are used for calibration. For each neutron an alpha particle is emitted. Thus, the number of 14 Mev neutrons can be determined and the sulfur counting rate calibrated. The calibration numbers for the counting systems used are as follows:

System	
End window geiger tube (Amperex 120N)	7.18×10^7 fast neutrons/cm^2 / count/min.
Methane gas flow counter	2.63×10^7 fast neutrons/cm^2 / count/min.
Thin wall aluminum counter with anticoincidence ring	4.51×10^6 fast neutrons/cm^2 / count/min.

Because the cross section for $S^{32}(n,p)P^{32}$ is small, provisions were made for counting weak samples. The 3-gram pellet normally used is made by compressing the flowers of sulfur at 10,000 psi in a 1-in. die. Three grams compressed in this way yields a pellet about 1/8 in. thick. This is practically infinitely thick for the 1.7 Mev beta ray from phosphorus. Since phosphorus is a pure beta emitter, thin window counters were used. Since there are no gamma rays, it is possible to count the activity of the sulfur pellets with an automatic sample changer (a hot sample in the changer will not raise the background significantly for a weak one in the counter). The automatic system has a resolving time of 540 μsec, so hot samples had to be counted in the manual methane-gas-flow counters (resolving time about 6 μsec). Each pellet was exposed in a container along with about 60 grams of flowers of sulfur. For the pellets that counted less than three times background (i.e., less than 80 cpm) in the automatic system, 40-gram cylinders were cast from the unprocessed sulfur. The activity in these cylinders was counted in the anticoincidence units (background 4 cpm) having a sensitivity 111 times as great.

$$\text{Sensitivity ratio} = \frac{\text{Cal. No. (end window)}}{\text{Cal. No. (anticoin.)}} \times \frac{\text{Background(end window)}}{\text{Background (anticoin.)}}$$

$$= \frac{7.18 \times 10^{7}}{4.51 \times 10^{8}} \times \frac{28}{4} = \frac{201.04}{18.04} = 111$$

Count-loss corrections were made using the factors appropriate to the system used. Count-rate corrections for variations in sample weight were computed, but the variation in weight requires a correction much smaller than the probable error in calibration; thus, weight corrections were not made. Corrected counting rates were extrapolated back to the irradiation time t_o by means of

$$CR_{t_o} = CR_t \, e^{\lambda s \, (t-t_o)}$$

where $\lambda s = \frac{0.693}{T_{\frac{1}{2}}} = 1.979 \times 10^{-3}$ per hour

CR_{t_o} = initial counting rate in counts per minute at t_o

CR_t = rate at time t in counts per minute

$T_{\frac{1}{2}}$ = 14.59 days, the half-life of P^{32}

The fast neutron flux (above 3 Mev) is then

$$nvt = K_{cal} \times CR_{t_o} \text{ neutrons per cm}^2.$$

2.4.3 Fission Detectors. The fissionable materials used were

plutonium-239, neptunium-237, and uranium-238. Approximate thresholds, cross sections, and sample weights were:

Sample	Threshold	Approximate Cross-Section (barns)	Sample Weight Approximate (gm)
Pu^{239}	(a) 200 ev	2.0	1.0
	(b) 1000 ev		
	(c) 4000 ev		
Np^{237}	0.75 Mev	1.5	0.050
U^{238}	1.5 Mev	0.43	0.66

(a) Surrounded by 1 cm thickness of elemental B^{10}
(b) Surrounded by 1.5 cm thickness of elemental B^{10}
(c) Surrounded by 2 cm thickness of elemental B^{10}

The effective threshold for the plutonium can be varied by changing the shield thickness. The samples were encased in copper or nickel foil.

In order to discriminate against the natural gamma-ray activity of the samples, scintillation counters with NaI (Tl) crystals were used with an integral pulse-height discriminator. The gamma rays were filtered through 1 cm of lead to use the increase in absorption coefficient with decreasing gamma ray energy to aid in the discrimination against lower-energy gamma rays and to prevent saturation of the crystal. Calibration of the detectors is effected by exposing 0.1 gm of plutonium to a known thermal flux in the ORNL graphite reactor. The flux is measured using gold foils. This gives the calibration for thermal neutrons. The known precise values for fast-neutron fission in the detector materials permit the calculation of fast-neutron calibration numbers by use of ratios (the thermal flux is shielded out when the detectors are used). For example calibration numbers used during Operation CASTLE were:

Sample	Time after exposure(hr)	Counting Apparatus Disc level(mev)	cpm for 10^{10}n on 1 gm
Pu	50	0.81	5
	100	0.81	3
U^{238}	50	0.34	7
	100	0.34	3
Np	50	0.62	10.2
	100	0.62	5.5

Since the calibrations are made by counting gamma rays above a certain energy (discriminator setting), the precision is a function of gain and discriminator stability. The counting systems must be standardized frequently. A Cobalt-60 source of about 1/2 microcurie is used. The discriminator and gain must be set to give the standard counting rate. The background activity has a long half life and, thus, represents the upper limit of sensitivity. Since the fission-fragment

activity falls off as an inverse power of t, the time after exposure, the sensitivity falls off with time lapse after exposure. For this reason early recovery is required. Calibrations must be made for specific counting times after exposure. Neptunium is acti ated by thermal neutrons giving Np^{238} with approximately 50 hours half life. The occurrence of this product disturbs the counting. Extra cadmium shielding must be used to minimize Np^{238} formation.

Chapter 3
RESULTS

The data are presented in the form of graphs. The graphs of the sulfur and fission data show nvt $\times R^2$ plotted as a function of R (the slant range) on semi-log graph paper. This type of plot results in a straight line for ranges greater than approximately 300 yd. At ranges shorter than this the curve tends to depart from the straight line. Insufficient correction for counting losses may account for some of the discrepancy and possibly a neutron build-up factor resulting from multiple scattering explains the rest.

The graphs of the gold data are plotted nvt $\times$ R versus R on semi-log graph paper. The resulting curve is a straight line beyond 500 yd. indicating that a 1/R dependence characteristic of the diffusion of the thermal neutron flux is descriptive of neutrons up to 0.3 ev energy. For ranges smaller than 500 yd, the curves deviate sharply from a straight line. This again may be due to the samples seeing an extended rather than a point source.

Listed on each graph are two parameters of interest. The e-fold distance is the distance over which the flux drops by a factor of 1/e, and is a measure of the mean free path for the neutrons measured by that particular type of detector. The R = 0 intercept is a rough measure of the neutron yield of the nuclear device. Relative neutron source strengths of the devices tested are given in Table 3.1.

Figures 3.1 through 3.10 show the results for gold, sulfur, and fission detectors for Shots 1, 9, and 10. On the graphs for Shot 10 are shown the values for Shot 9 scaled from the Nevada Test Site to 36,620 ft altitude, by means of the following scaling formulas:

$$\text{Distance (altitude)} = \text{Distance (NTS)} \times \frac{\rho\,(\text{NTS})}{\rho(\text{altitude})}$$

$$\text{Flux (altitude)} = \text{Flux (NTS)} \times \left[\frac{\rho(\text{altitude})}{\rho(\text{NTS})}\right]^2$$

where ρ is the ambient air density. Moisture-content corrections amount to a fraction of a percent and were not used. Density corrections using the method of Weidler and Ward, (SWR 54-4 May 1954 (S)), for scaling the Shot 9 data to Shot 10 altitude should be made to account for the lower average density along the path to the more distant and higher canisters which consequently show a somewhat higher flux. This correction would bring the scaled Shot 9 data more nearly into coincidence with the Shot 10 data. This correction is less than the probable error of measurement for all but the three most distant canisters. Neutron spectrum histograms are presented in Figure 3.31. Composite neutron data is given in 3.30.

The figures

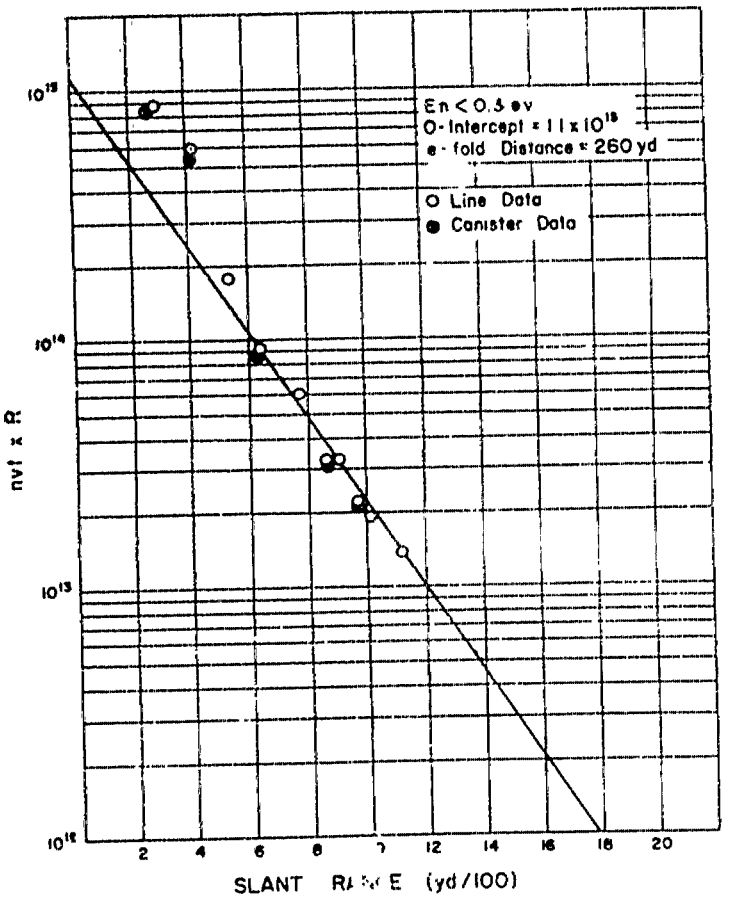

Fig. 3.1 - Shot 1, Slow (gold) Neutron Data (nvt x R vs R)

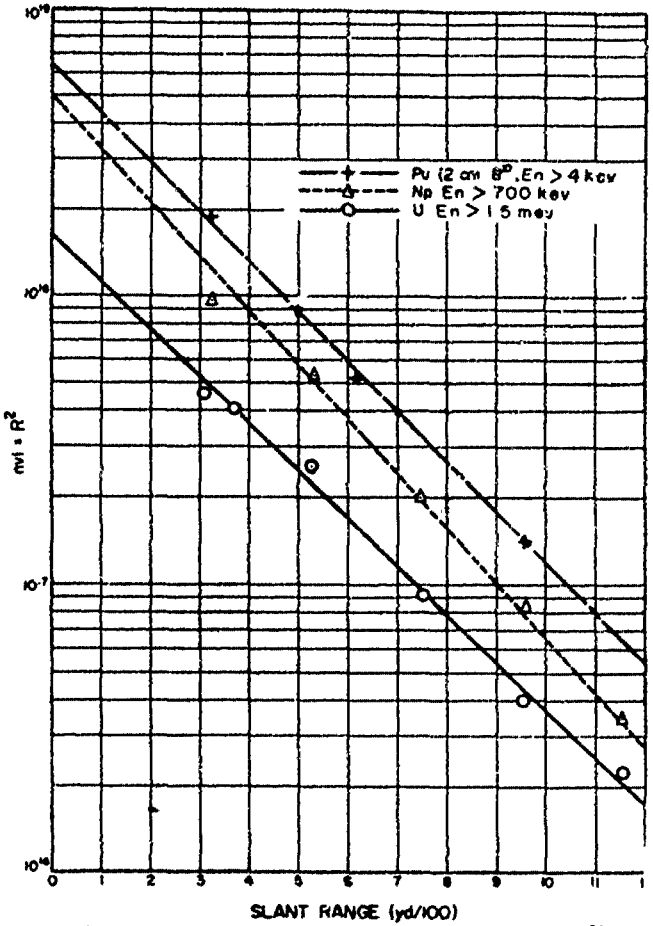

Fig. 3.3 - Shot 1, Intermediate Neutron Data - Pu with 2 cm B^{10}, 4 kev Threshold; N_p; and U^{238}; (nvt x R^2 vs R)

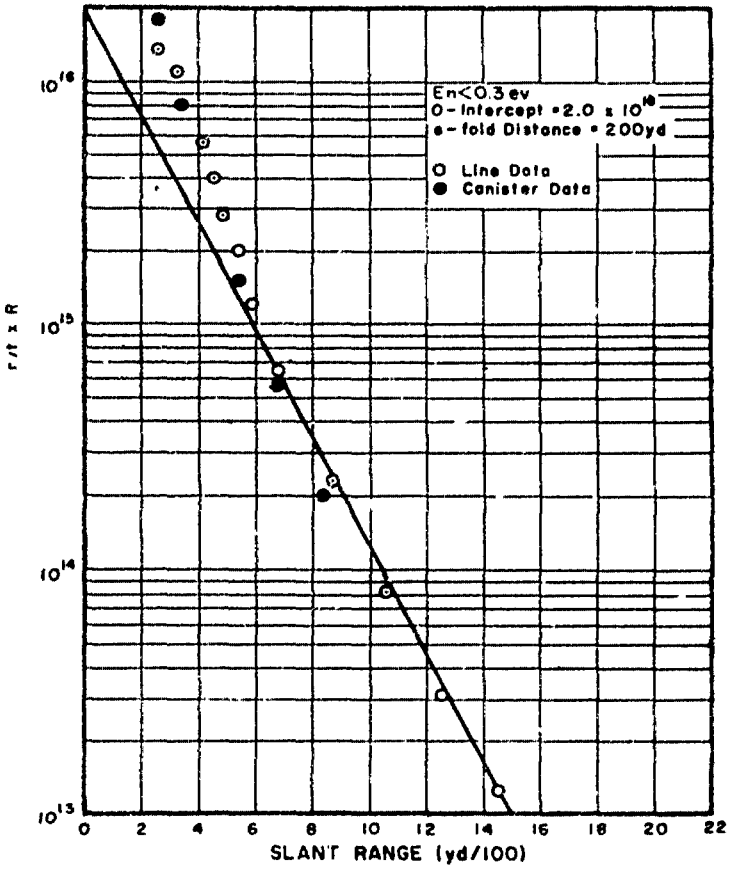

Fig. 3.4 - Shot 9, Slow (gold) Neutron Data (nvt x R vs R)

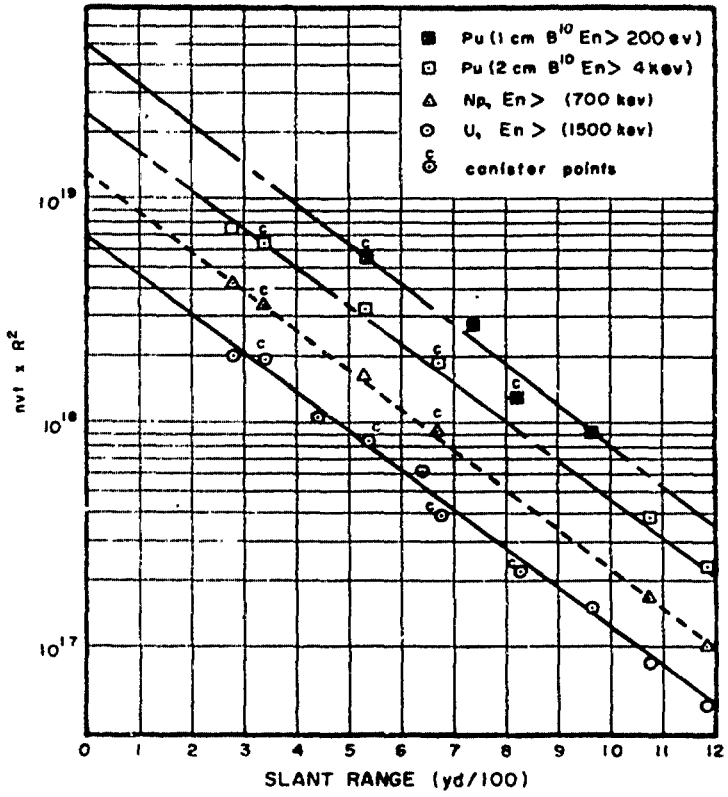

Fig. 3.6 - Shot 9, Intermediate Neutron Data - Pu with 1 cm B^{10}, 200 ev Threshold; Pu with 2 cm B^{10}, 4 kev Threshold; Np; U^{238} (nvt x R^2 vs R)

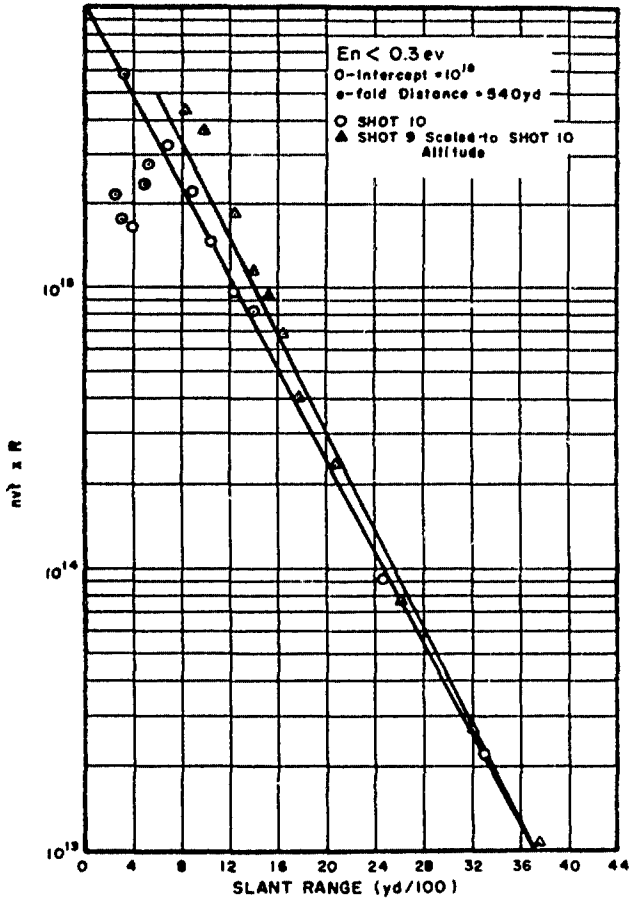

Fig. 3.7 - Shot 10, Slow Neutron Data and Shot 9 Scaled to Shot 10 Altitude (nvt x R vs R)

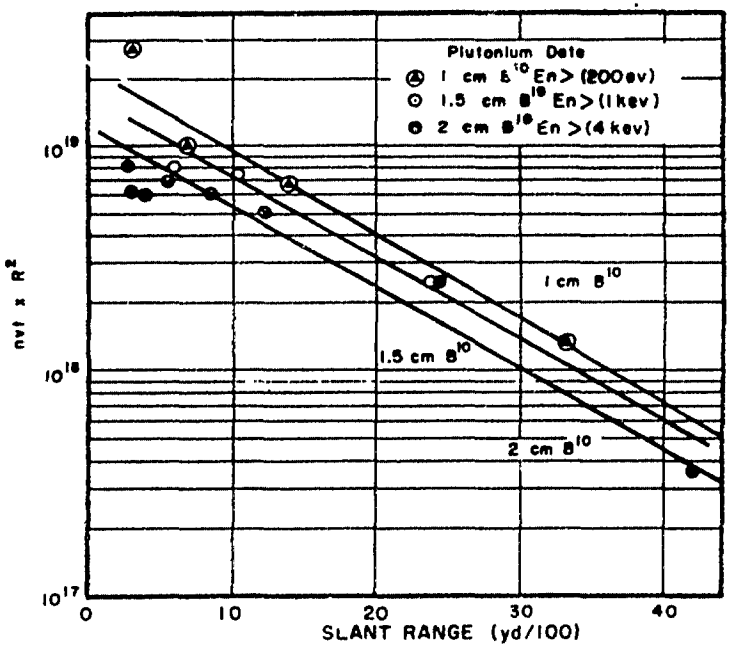

Fig. 3.8 - Shot 10, Intermediate Neutron Data; Pu with 1 cm B^{10}, 200 ev Threshold; Pu with 1.5 cm B^{10}, 1 kev Threshold; Pu with 2 cm B^{10}, 4 kev; (nvt x R^2 vs R)

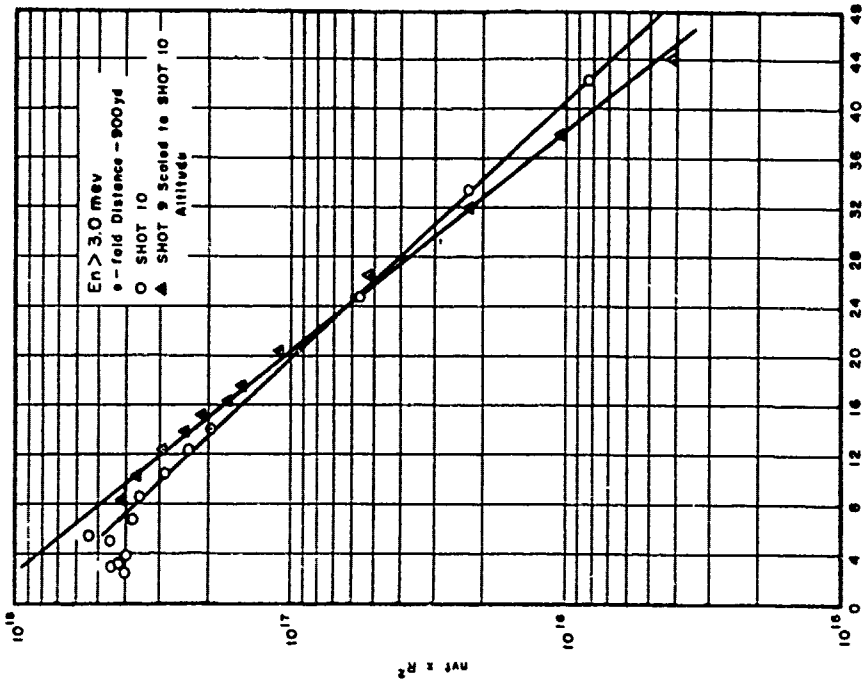

Fig. 3.10 - Shot 10, Fast (unfilter) Dosage Data and Shot 9 Scaled to Shot 10 Altitude (nvt x R² vs R)

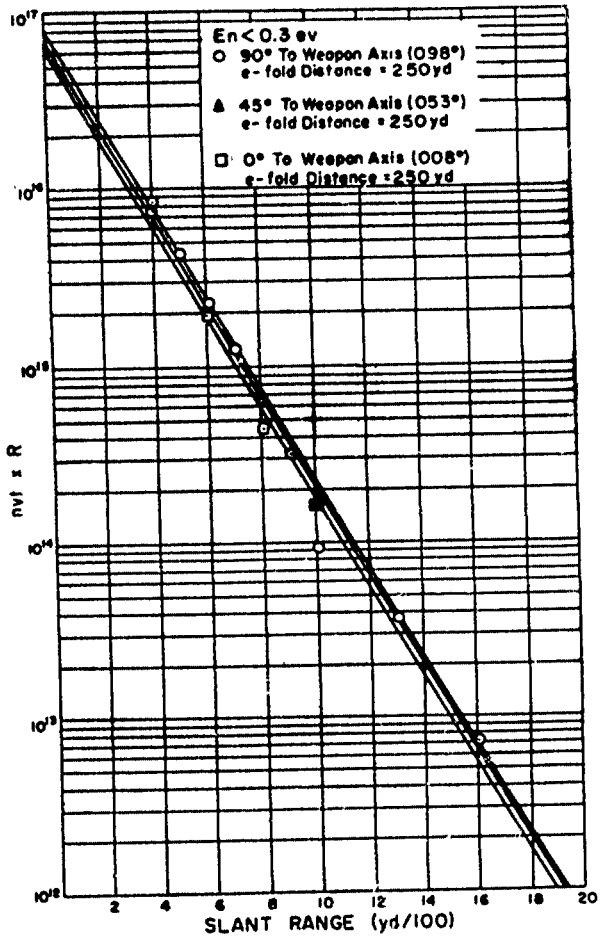

Fig. 3.11 - Shot 3, Slow (gold) Neutron Data (nvt x R vs R)

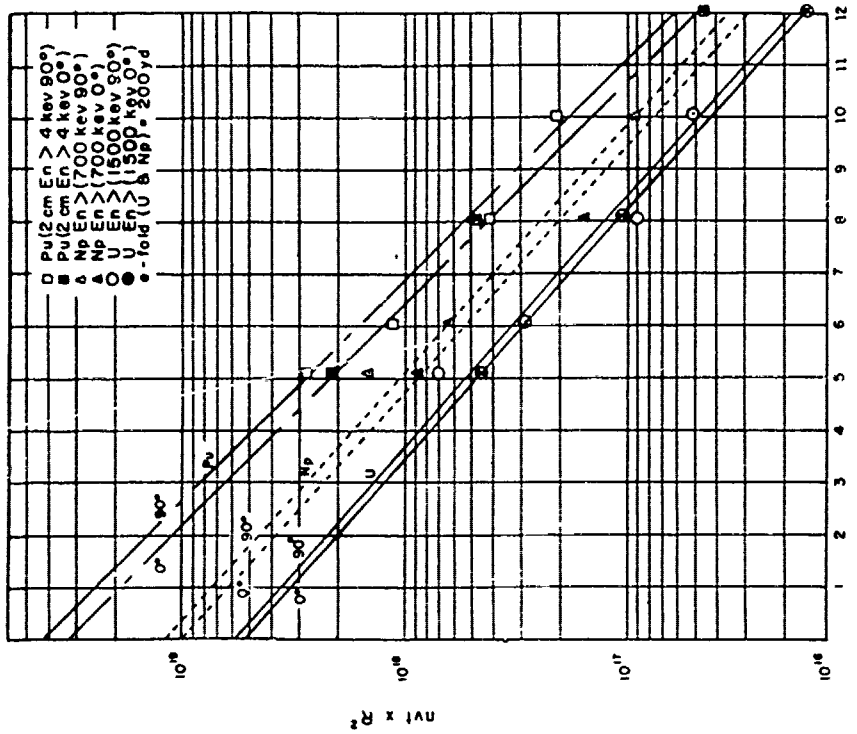

Fig. 3.12 - Shot 11, Intermediate Neutron Data Fu, Np, U, (nvt x R^2 vs R)

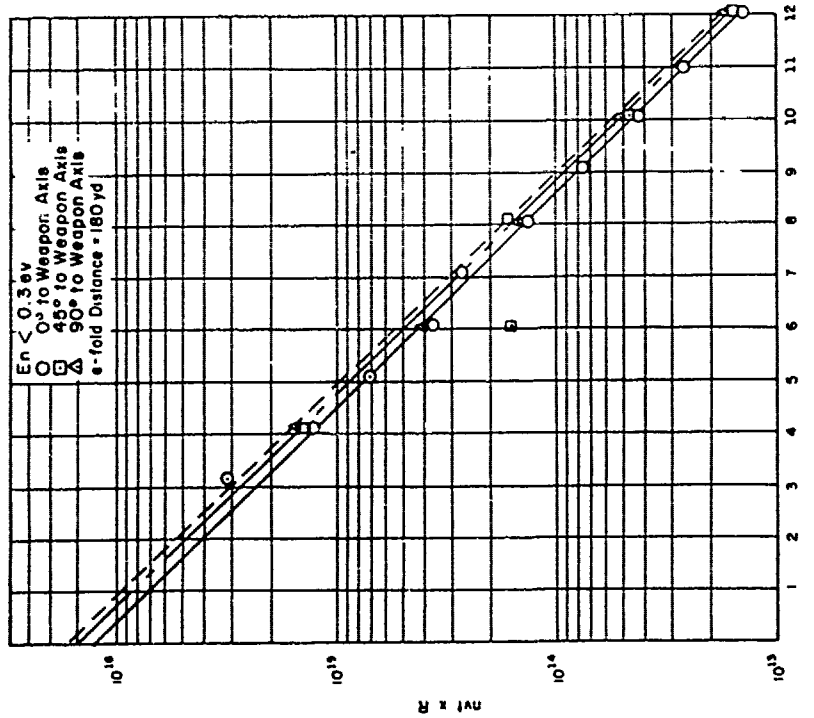

Fig. 3.13 - Shot 11, Slow (gold) Neutron Data (nvt x R vs R)

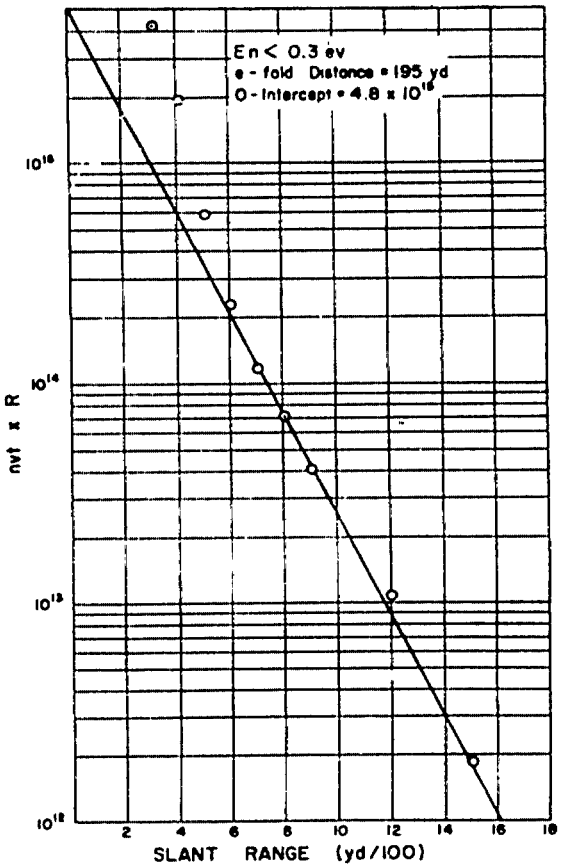

Fig. 3.16 - Shot 2, Slow (gold) Neutron Data (nvt x R vs R)

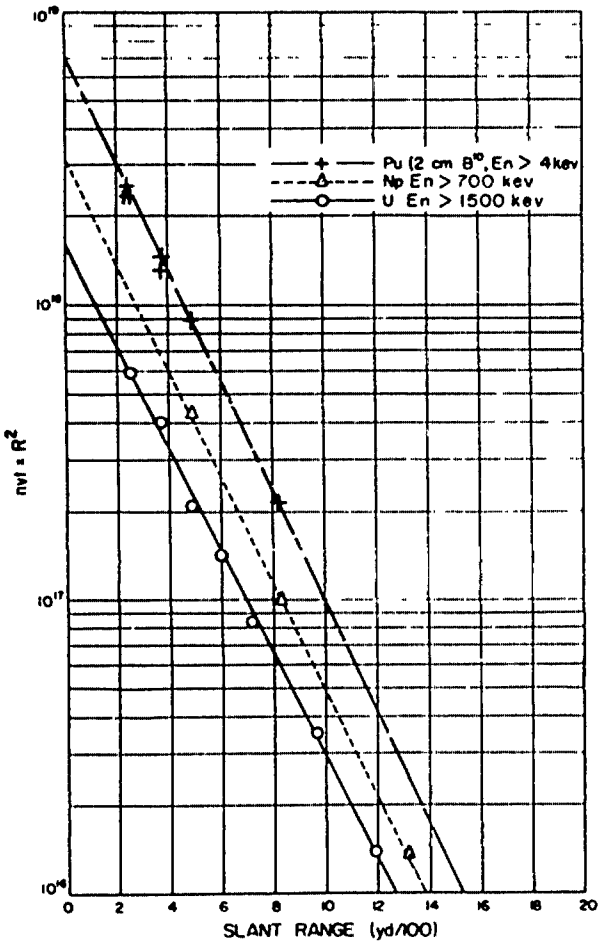

Fig. 5.17 - Shot 2, Intermediate Neutron Data Pu, Np, U^{238}; (nvtxR^2 vs R)

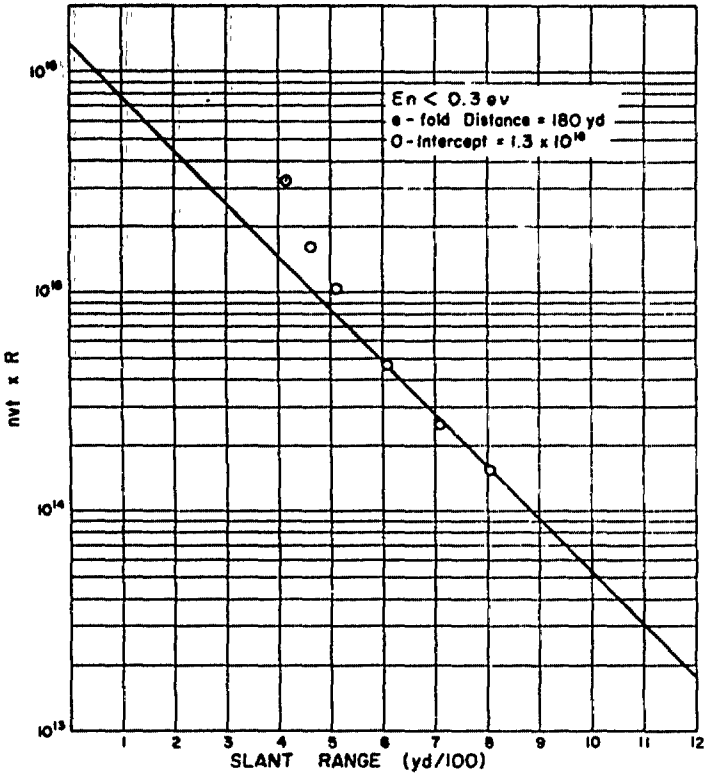

Fig. 3.19 - Shot 5, Slow (gold) Neutron Data (nvt x R vs R)

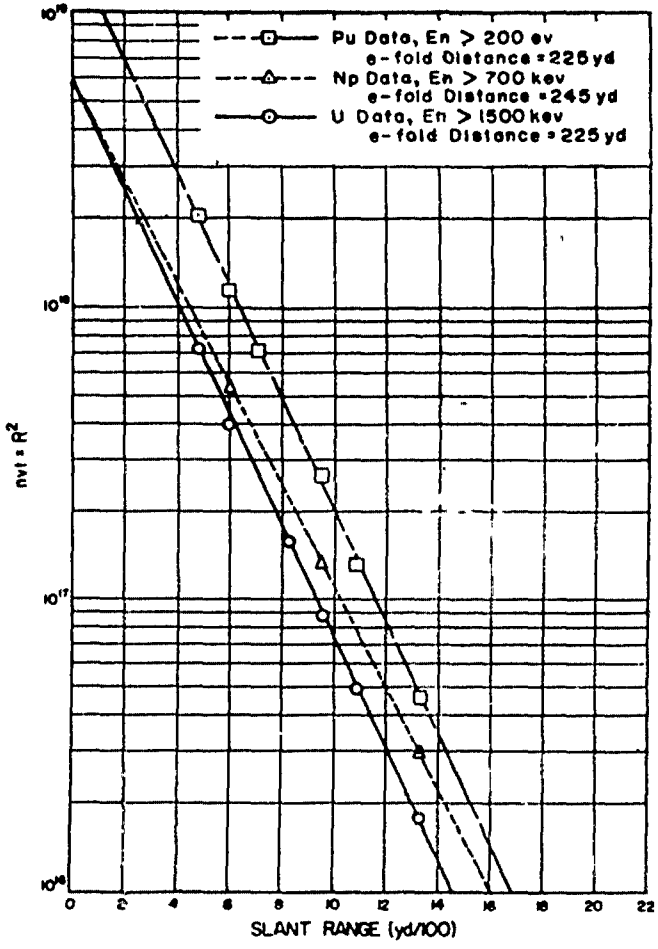

Fig. 3.20 - Shot 5, Intermediate Neutron Data; Pu, Np, U^{238}; ($nvt \times R^2$ vs R)

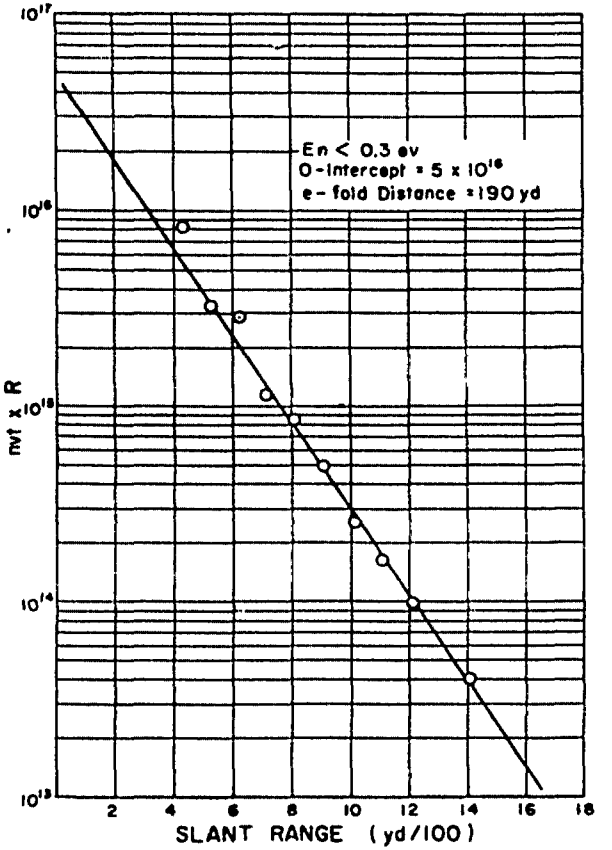

Fig. 3.22 – Shot 6, Slov (gold) Data (nvt x R vs R)

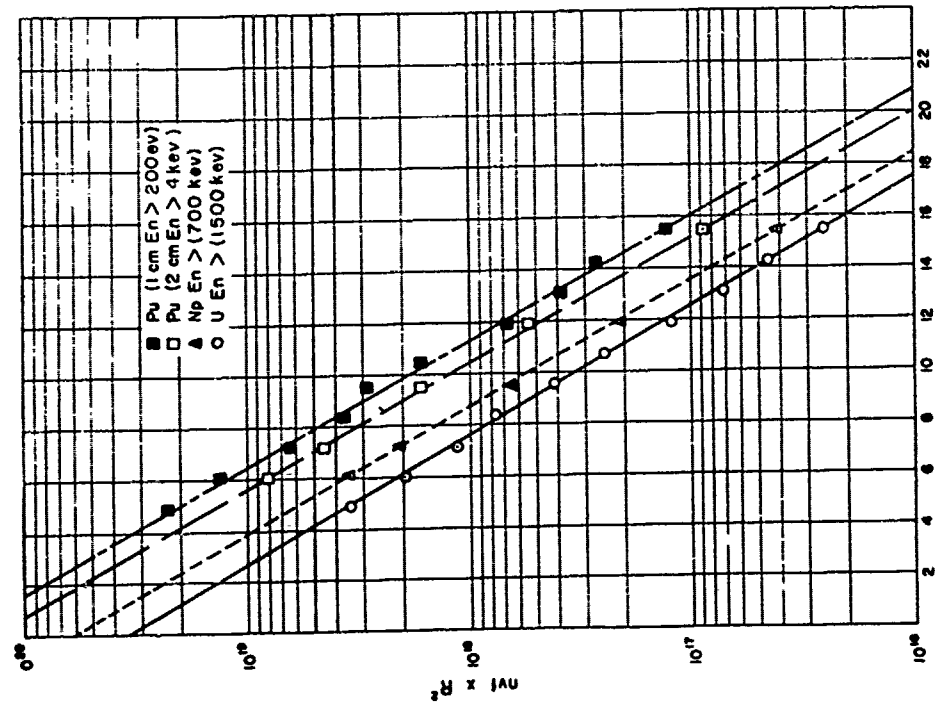

Fig. 3.23 - Shot 6, Intermediate Neutron Data (Pu, Np, U^{238}) (n/cm² vs R)

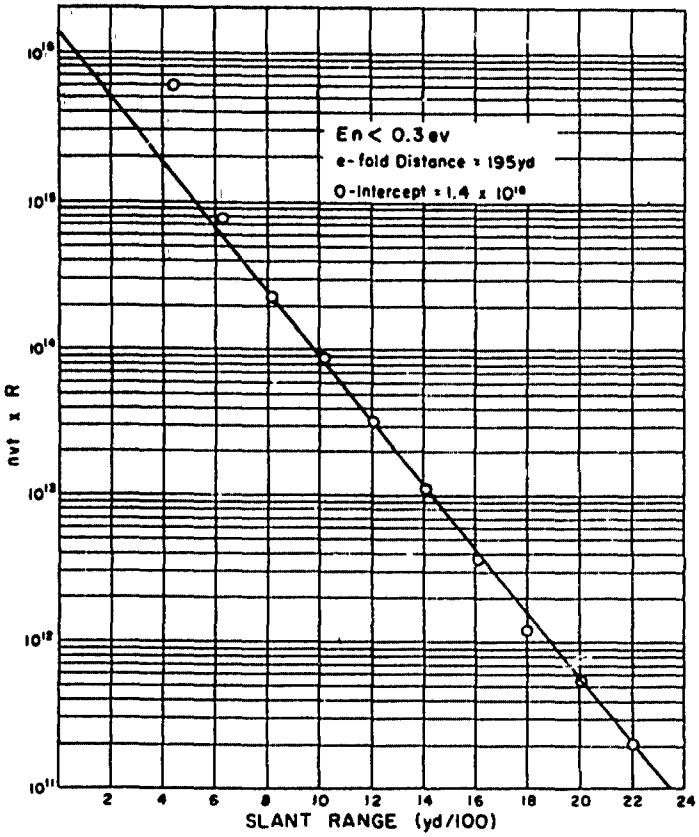

Fig. 3.25, Shot 8, Slow (gold) Neutron Data, (nvt x R vs R)

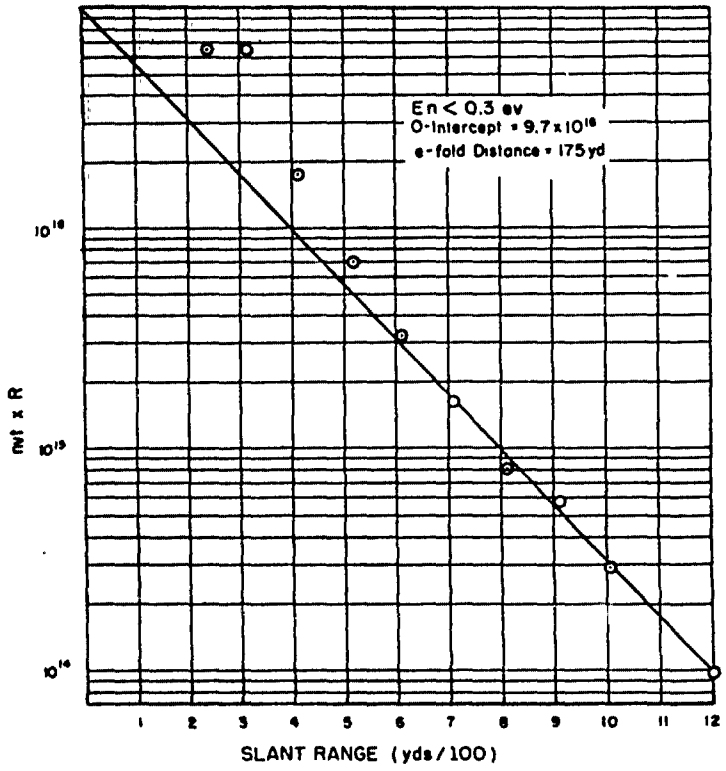

Fig. 3.27 - Shot 12, Slow (gold) Data (nvt x R^2 vs R)

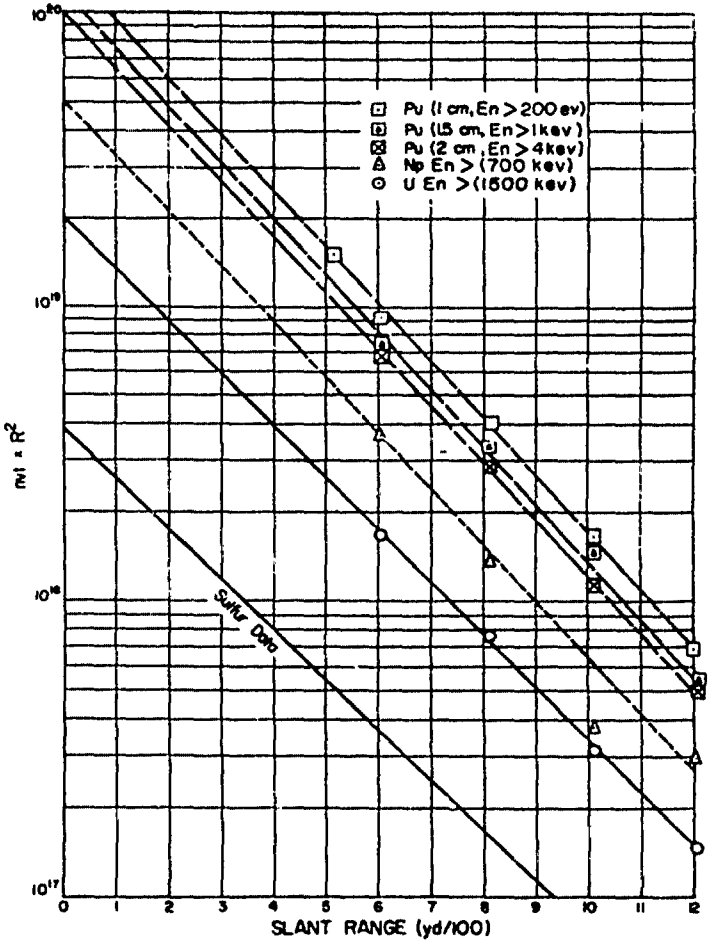

Fig. 3.28 - Shot 12, Intermediate Neutron Data, Pu,Np,U^{238},(nvtxR^2 vs R)

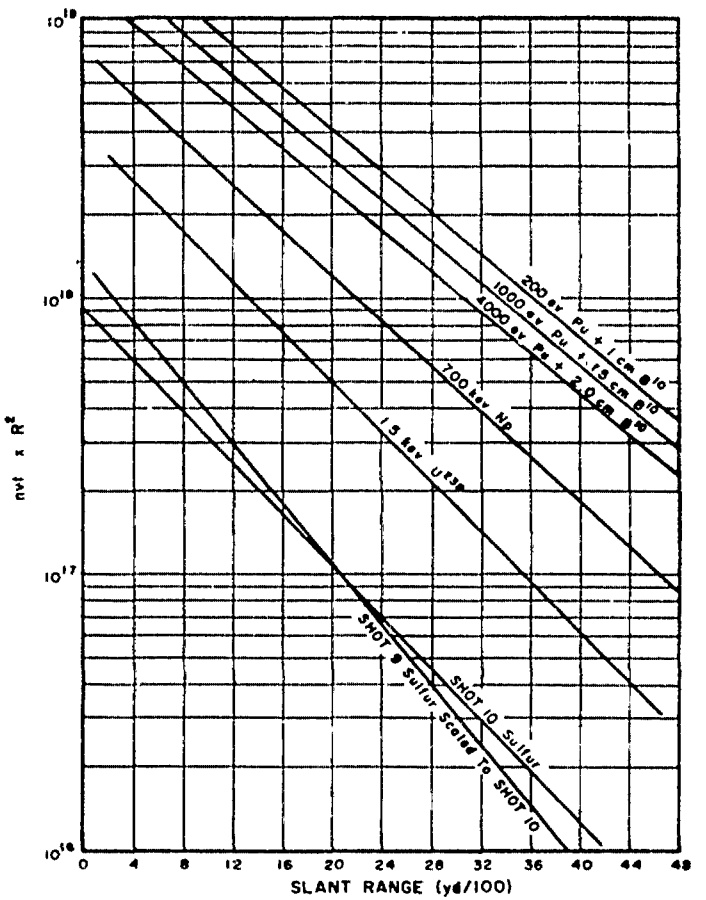

Fig. 3.20 - Shot 10 (HA) Composite Neutron Data (nvt x R^2 vs R)

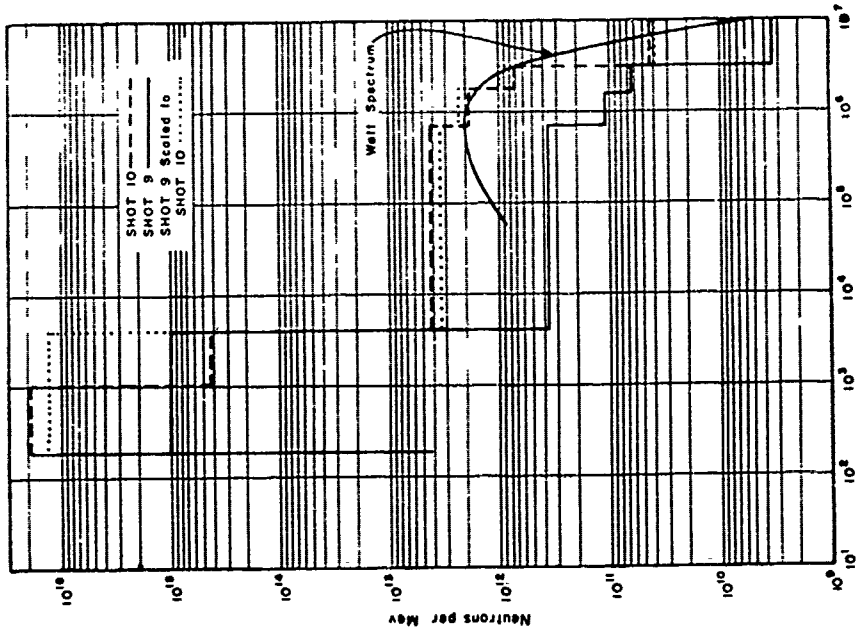

Fig. 3.11 - Neutron Histogram at 1000 yd.

(3.11 through 3.15) show three curves each, with the lower curve in each case being data from the line along the axis of the device. The fluxes along the 45° and 90° approximately are successively higher.

Figures 3.16 through 3.24 show the results for Shots 2, 5, and 6.

Figures 3.25 and 3.26 give the results from the gold and sulfur detectors at Shot 8; no fission detectors were exposed.

Figures 3.27, 3.28, and 3.29 show the gold, sulfur, and fission-detector data for Shot 12. This line was installed to provide a flux and spectrum measurement for comparison with data taken in field fortifications by Project 2.7.

Chapter 4
CONCLUSIONS and RECOMMENDATIONS

The effects of weapons design, whether a given device was of the spherical implosion or linear implosion type, the mechanical construction of a device, and type of fuzing and "case" instrumentation all combine to confuse a comparative neutron source strength figure. However, in cases where the basic design of several devices was the same (as with Shots 3 and 11), or where the main purpose of several shots was to study various cases for a given type of core, some comparison is valid and of interest. For this reason, within the categories of shots set up, the devices are comparable to one another.

In the presentation of neutron flux data it is difficult to attach significance to the variation in intensity with range. For fast neutrons the inverse square law and exponential absorption are assumed. The extrapolation of a plot of nvt $\times R^2$ versus R on semi-log paper intercepts the ordinate axis at the so-called zero intercept. The magnitude of this intercept is useful along with the e-folding distance only in constructing the data curve from these pieces of information. The discrepancy between the zero intercept interpreted as source strength and the neutron yield calculated by other means has been noted. Assuming that source calculations and detector calibrations are sensibly correct, the discrepancy must be attributable to the interpretation of absorption and scattering in the medium. Threshold detectors are "poor" geometry detectors. The concept of an absorption coefficient should be applied only to "good geometry" or "collimated" systems. The absorption coefficient in good geometry is

$$\mu = \mu_a + \mu_i + \mu_e$$

where μ_a refers to neutrons lost by absorption resulting in some nuclear reaction as (n,α), (n,p) or (n,γ), μ_i refers to neutrons scattered out of the beam by inelastic processes, and μ_e refers to neutrons scattered out of the beam by elastic processes. In good geometry the detector flux is

$$F = \frac{S}{4\pi R^2} e^{-\mu R},$$

S is the source strength. The measured flux F_o near the weapons is usually written

$$F_o = \frac{S}{4\pi R^2} e^{-R/L}$$

where L is the e-folding distance, $1/L = \mu_A$. It may be assumed that μ_a is approximated by μ_A. Then one could write

$$F_o = \frac{S}{4\pi R^2} e^{-[\mu - (\mu_i + \mu_e)]R}$$

and say that

$$S = 4\pi R^2 F_o e^{[\mu - (\mu_i + \mu_e)]R}$$

However, μ_A is not simply related to μ_a. The coefficient μ_A is the coefficient for absorption somewhere in the sphere of radius R. The value of μ_A can be estimated only by means of a Monte Carlo calculation that follows each neutron to its capture or passage through the sphere. The coefficient μ_a gives the "good" geometry absorption for the direct path. Thus $\mu_a < \mu_A < \mu$.

The expression for S above is only an approximation, but it does indicate that the source strength estimated from experimental data is too large and should be reduced by a factor phenomenologically similar to

$$e^{-(\mu_e + \mu_i)R}$$

Calculations of the "in scatter" from singly scattered neutrons, performed for HARDTACK indicate that this "in scatter" is comparable to the direct flux at ranges of about 800 yd from HA. Multiply scattered neutrons will make this factor still larger.

It seems that the geometry consideration could explain the discrepancy. A detailed calculation would be required to get dependable numbers. A Monte Carlo calculation accounting for multiple scattering is required to determine whether or not scattering is the only source of the discrepancy.

The custom of plotting slow neutrons as nvt × R versus R on a semi log plot derives from diffusion theory which says that the intensity of thermal neutron flux falls off as 1/R for a point source. Other functional presentations of the data could be used. The methods used in this and previous reports are for convenience in presentation.

Since the presentation chosen is not justified except for convenience, the curves through the points were not fitted by the method of least squares. The lines were drawn considering the greater dependability of points corresponding to activities small enough to require negligible count loss correction and large enough to require negligible background correction.

In the graphs following, E_n is the neutron energy.

The gold and sulfur data for Shot 1(Figures 3.1 and 3.2) show irregular points and greater-than-normal e-fold distances. Stations used for this shot lay on a curved line about ground zero. Since the angles to the stations are not known, it is not possible to correct for bomb error in order to determine the correct e-fold distance and flux level. Since the circular error was substantial (437 ft) for this shot, the

close-in points require a considerable correction relative to the more distant points, which will make the curves steeper.

The same holds true for Shot 9, but the error is much less, the circular error being only 113 ft. However, in this case the corrections for bomb error have been made and the e-fold distance is about right and the range = 0 intercept is comparable to that of Shot 10.

Shots 9 and 10 appear to be very-nearly alike as neutron sources. If the yields were equal, the neutron flux per kiloton of yield is approximately equal.

Data for Shot 10 show wide fluctuations for all detectors at close range. It will be noted that there is a minimum in the neutron-detector data at 400 yd range from Shot 10. The anhydrous-chloroform gamma-ray dosimeters give a maximum at this range for gamma rays. A cursory examination of the phosphate-glass dosimeters indicates a gamma-ray minimum at about 300 yd and a maximum at about 350 to 400 yd. Because of the inconsistency of the data in the first 500 yd from Shot 10, no satisfactory interpretation in this region has been found. The orientation of the canisters was determined without difficulty and the properly oriented samples were used for Shot 10 data. Figure 3.30 gives the composite Shot 10 data.

[redacted] asymmetry in the neutron flux was observed during Shots 3 and 11. [redacted] the weapon is approximately 30 percent higher than the flux along the [redacted] Both weapons yielded higher flux than expected. Figures 3.11 and 3.12 present the data that show the asymmetry. The 900 and 1,000 yd stations on the 90° line give bad data points for both the gold and sulfur detectors. This is attributed to a shadowing effect from structures near these stations. Because the area was clean after the shot the cause of the bad points could not be determined. From the best data the e-folding distance appears to be about 250 yd.

The neutron yield from Shot 12 was near expectations. Figure 3.28 gives the composite neutron data.

The use of threshold detectors in the intermediate energy range makes it possible to show the importance to dose calculations of the knowledge of the spectrum distribution. The neutron flux in the intermediate region is surprisingly high. The histogram, Figure 3.31, shows graphically (Shot 9 and Shot 10 data) that relating neutron dose to sulfur flux leads to erroneous results. The solid curve on Figure 3.31 is the "Watt spectrum" normalized to fit the data at 1 Mev. For fission neutrons one expects the spectrum amplitude to drop for energies below 1 Mev until the thermal region is reached. Although the slow-neutron flux (gold) is not shown in Figure 3.31, the "bomb thermals" are, i.e., the histogram blocks lying between 200 ev and 4,000 ev represent the neutrons at bomb thermal energy (in the neighborhood of 1,000 ev).

It is concluded that the predictions on radiation effects [redacted] are essentially correct. The Shot 10 results are within predicted limits. The data from Shot 9 scales to Shot 10 data within the precision of the flux measurements. Shot 3 and 11, the [redacted] gave [redacted] asymmetry --, [redacted] The results obtained with

detectors supplied to Project 2.7 for structure shielding studies should be sought in the Project 2.7 report.

Recommendations must be limited to further test work since recommendations concerning military weapons designed from the devices tested is an operational responsibility. Because it has been shown that radiation effects at high altitude produce lethal damage at considerable range, it is recommended that nuclear radiation measurements be included in future tests of weapons detonated at high altitude.